

# Effects of counterion fluctuations in a polyelectrolyte brush

C.D. Santangelo<sup>1</sup> and A.W.C. Lau<sup>2</sup>

<sup>1</sup>*Department of Physics, University of California, Santa Barbara, CA 93106, USA*

<sup>2</sup>*Department of Physics and Astronomy, University of Pennsylvania, Philadelphia, PA 19104, USA*

(Dated: June 19, 2018)

We investigate the effect of counterion fluctuations in a single polyelectrolyte brush in the absence of added salt by systematically expanding the counterion free energy about Poisson-Boltzmann mean field theory. We find that for strongly charged brushes, there is a collapse regime in which the brush height decreases with increasing charge on the polyelectrolyte chains. The transition to this collapsed regime is similar to the liquid-gas transition, which has a first-order line terminating at a critical point. We find that for monovalent counterions the transition is discontinuous in theta solvent, while for multivalent counterions the transition is generally continuous. For collapsed brushes, the brush height is not independent of grafting density as it is for osmotic brushes, but scales linear with it.

PACS numbers: 61.25.Hq, 61.20.Qg

## I. INTRODUCTION

Recently, correlation effects in electrostatics of highly charged macroions in aqueous solution have received a great deal of attention (see Refs. [1, 2, 3], for recent reviews). These effects give rise to interesting phenomena that are not contained in the mean-field Poisson-Boltzmann (PB) theory [4], such as charge inversion [1] and like-charge attraction [2, 3]. One plausible origin of the attraction comes from fluctuations of the counterion density that become correlated leading to a long-range attraction that is similar to van der Waals forces [5, 6, 7]. Counterion fluctuations might have important effects on the conformation of highly-charged polyelectrolytes [8, 9]. In this paper, we study the effects of counterion fluctuations in a polyelectrolyte brush, where these effects are thus expected to be important.

A polyelectrolyte brush consists of a high density of charged polymers with one of their ends grafted to a surface (see Fig.1). Because of their technological applications, such as enhanced stabilization against colloidal flocculation, they have been extensively studied in the past both theoretically [10, 11, 12, 13, 14, 15, 16] and experimentally [17, 18, 19, 20]. Pincus [12] studied polyelectrolyte brushes, based on the Alexander-deGennes approximation [21], where monomer density is assumed to be constant up to the brush height, and mean-field PB theory for the electrostatic interaction between the charged monomers and the counterions. The brush height, a quantity that is accessible to experiments, is then determined self-consistently by minimizing the total free energy of the brush. In a theta solvent, it simply consists of the elastic energy arising from stretching the chains and the electrostatic (mean-field) free energy. In this picture, there are basically two regimes – weak-charging and strong-charging (osmotic) regimes. In the weak-charging regimes, the counterions are diffuse and the brush height scales with the degree of polymerization of the charged polymer  $N$ , like  $h \sim N^3$ . In the osmotic regime, most of the counterions are trapped inside the

brush, whose osmotic pressure (which tends to increase the brush height) is balanced by elasticity of the chains (which tends to decrease the brush height). In this limit, the chains are stretched and the brush height,  $h \sim N$  and is independent of the grafting density. In later studies, this mean-field electrostatic picture has been extended to poor solvent, where a first-order collapse transition was predicted [13], to the quasi-neutral regime where excluded volume effects are important [14], and to the self-consistent field theory which goes beyond the Alexander-deGennes approximation [15].

Early experiments on moderately charged polyelectrolyte brush show that the above theory is reasonably valid [17, 18, 19, 20]. However, recent experiments on highly charged brushes have shown behavior that cannot be described within mean-field PB theory, especially in the presence of multivalent counterions. Experiments on the normal forces between two brushes [22] have seen decreases of brush height with multivalent salt and condensation beyond that predicted by Manning theory. There is also evidence of attractive interactions between the brushes [23]. In addition, Bendejacq *et al.* [24] have observed a regime in highly charged cylindrical brushes of annealed polyelectrolytes characterized by a continuous decrease in brush height with increasing brush charge. The nonmonotonic behavior of the brush height occurs even with monovalent counterions and there exists a novel scaling relation between the brush height and the concentration of added salt. Finally, a recent simulation [25] also finds enhanced condensation and a collapsed brush regime even with monovalent counterions. It also shows for large values of grafting density, the brush height does not follow any of the scaling laws above.

These observations strongly suggest that counterion correlation effects are important in highly charged brushes, especially in the presence of multivalent ions. In Ref. [26], Csajka *et al.* developed a scaling theory describing strongly charged brushes using the so-called box model. In this model, the chains in the brush are assumed to be equally stretched and the counterions are assumed

to be distributed with constant density. In addition to the mean-field electrostatic free energy, a counterion fluctuation energy, estimated using the Debye-Hückel free energy of electrolytes [27], is added to reflect correlation effects. This new term tends to decrease the brush height. This model predicts a collapsed regime in which the Debye-Hückel fluctuation pressure is balanced by the second virial pressure. The transition between the osmotic brush and the collapsed brush is predicted to be first order.

In this paper, we develop a theoretical framework that goes beyond scaling theory and systematically study the role of counterion density fluctuations in the absence of added salt. This is done by employing a field theory for the counterion contribution to the free energy and *systematically* expanding about the mean field counterion density to second order in the fluctuations [7, 29]. The chains are treated within the Alexander-deGennes approximation of equal stretching and constant monomer density. We find that for strongly charged brushes, there is a collapse transition in which the brush height decreases with increasing charge on the polyelectrolyte chains. Unlike the scaling theory [26], we find that the transition is similar to the liquid-gas transition with a line of first-order phase transition terminating at a critical point. Surprisingly, the valence of the counterions plays an important role: the transition to the collapse regime is discontinuous for monovalent counterions, while it is continuous for multivalent counterions. Furthermore, for collapsed brushes, we find that the brush height is no longer independent of the grafting density, as in osmotic brushes, but scales linearly with it. Our results are expected to be relevant to ongoing experimental studies in polyelectrolyte brushes and our framework can be easily generalized to study the important case of the interaction between two highly-charged brushes..

The organization of the paper is as follows: In section II, we review the expansion about the PB mean field theory in order to establish notation. In section III, we specialize to the case of a single polyelectrolyte brush and calculate the phase diagram in both theta solvent

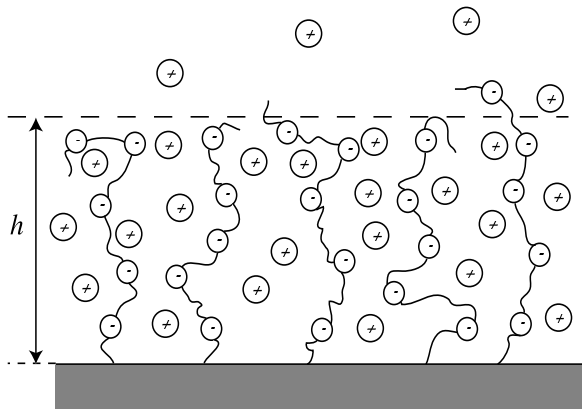


FIG. 1: A schematic picture of a polyelectrolyte brush.

and good solvent. Finally, in section IV, we discuss the meaning and limitations of our results. The detailed calculation of the fluctuation effects have been left to the Appendix.

## II. COUNTERION FREE ENERGY

In this section, we briefly review the theoretical method that allows us to compute in a rigorous fashion the total electrostatic free energy that includes fluctuation contributions from the counterions. The details can be found elsewhere [28, 29]. The idea is to map the partition function of a system of counterions interacting among themselves and with a fixed distribution of charges to a field theory characterized by an effective Hamiltonian. We can then systematically expand about its saddle-point solution, which corresponds to nothing but the mean-field PB approximation, and calculate the fluctuation contributions to the lowest order. While the discussion here is general, we will apply this formulation to our model of polyelectrolyte brush in Sec. III.

Consider the primitive model where a system of  $N_c$  point-like charged particles of charge  $-Ze$  (where  $Z$  is the valence) and external fixed charges with charge density  $\sigma(\mathbf{x}) = en_f(\mathbf{x})$ , immersed in an aqueous solution with dielectric constant  $\epsilon$ . The electrostatic energy for this charged system is

$$\beta E_{N_c} = Z^2 l_B \sum_{j>k}^{N_c} \frac{1}{|\mathbf{x}_j - \mathbf{x}_k|} - \sum_{j=1}^{N_c} \phi(\mathbf{x}_j), \quad (1)$$

where  $\phi(\mathbf{x}) = Z l_B \int d^3 \mathbf{x}' \frac{n_f(\mathbf{x}')}{|\mathbf{x} - \mathbf{x}'|}$  is the “external” electric potential from the fixed charge distribution and  $l_B \equiv \frac{e^2}{\epsilon k_B T} \approx 7 \text{ \AA}$  is the Bjerrum length in water at room temperature,  $k_B$  is the Boltzmann constant, and  $T$  is the temperature. The partition function is

$$Z_{N_c}[\phi] = \frac{1}{N_c!} \prod_{i=1}^{N_c} \int \frac{d^3 \mathbf{x}_i}{a^3} \exp(-\beta E_{N_c}), \quad (2)$$

where  $a$  is the molecular size of the counterions and  $\beta \equiv 1/(k_B T)$ . The partition function of Eq. (2) can be mapped into a field theory, by switching to the grand canonical ensemble. We introduce a chemical potential  $\mu$  (in units of  $k_B T$ ) and express the grand partition function as

$$\mathcal{Z}_\mu[\phi] = \sum_{N_c=0}^{\infty} e^{\mu N_c} Z_{N_c}[\phi]. \quad (3)$$

After a Hubbard-Stratonovich transformation, we obtain the functional representation for the system of charges in an external field:

$$\mathcal{Z}_\mu[\phi] = \mathcal{N}_0 \int \mathcal{D}\psi e^{-\mathcal{S}[\psi, \phi]}, \quad (4)$$

$$\begin{aligned} \mathcal{S}[\psi, \phi] &= \int \frac{d^3\mathbf{x}}{\ell_B} \left\{ \frac{1}{2} \psi(\mathbf{x}) [-\nabla^2] \psi(\mathbf{x}) - \kappa^2 e^{i\psi(\mathbf{x}) + \phi(\mathbf{x})} \right\} \\ &\equiv \int d^3\mathbf{x} \mathcal{H}[\psi, \phi], \end{aligned} \quad (5)$$

where  $\ell_B = 4\pi l_B Z^2$ ,  $\kappa^2 = \rho_0 \ell_B$ ,  $\rho_0 = e^\mu / a^3$ , and  $\mathcal{N}_0^{-2} \equiv \det[-\nabla_{\mathbf{x}}^2]$  is the normalization factor. The saddle point,  $\psi_0(\mathbf{x})$ , given by  $\left. \frac{\delta \mathcal{S}}{\delta \psi(\mathbf{x})} \right|_{\psi=\psi_0} = 0$ , is determined by the equation

$$\nabla^2 [i\psi_0(\mathbf{x})] = \kappa^2 e^{i\psi_0(\mathbf{x}) + \phi(\mathbf{x})}, \quad (6)$$

which after introducing the mean-field potential,  $\varphi(\mathbf{x}) = -i\psi_0(\mathbf{x}) - \phi(\mathbf{x})$ , becomes

$$\begin{aligned} \nabla^2 \varphi(\mathbf{x}) + \kappa^2 e^{-\varphi(\mathbf{x})} &= -\nabla^2 \phi(\mathbf{x}) \\ &= \frac{\ell_B}{Z} n_f(\mathbf{x}), \end{aligned} \quad (7)$$

which is the Poisson-Boltzmann equation. This equation will be examined more closely in Sec. III A for our model of polyelectrolyte brush to be introduced in Sec. III.

To obtain the free energy for the counterions at the mean-field level, we note that it is related to the Gibbs potential  $\Gamma_0[\phi] \equiv \mathcal{S}[\psi_0, \phi]$  by a Legendre transformation:

$$\beta F_0(n) = \Gamma_0[\phi] + \mu \int d^3\mathbf{x} \rho_0(\mathbf{x}), \quad (8)$$

where  $\rho_0(\mathbf{x})$  is the mean-field free counterion density given by

$$\rho_0(\mathbf{x}) = \rho_0 e^{i\psi_0(\mathbf{x}) + \phi(\mathbf{x})}. \quad (9)$$

To capture correlation effects, we expand the action  $\mathcal{S}[\psi, \phi]$  about the saddle-point,  $\psi_0(\mathbf{x})$ , to second order in  $\Delta\psi(\mathbf{x}) = \psi(\mathbf{x}) - \psi_0(\mathbf{x})$ :

$$\begin{aligned} \mathcal{S}[\phi, \psi] &= \mathcal{S}[\phi, \psi_0] \\ &+ \frac{1}{2} \int d^3\mathbf{x} \int d^3\mathbf{y} \Delta\psi(\mathbf{x}) \hat{\mathbf{K}}(\mathbf{x}, \mathbf{y}) \Delta\psi(\mathbf{y}) + \dots, \end{aligned} \quad (10)$$

where the differential operator

$$\hat{\mathbf{K}}(\mathbf{x}, \mathbf{y}) \equiv \left[ -\nabla_{\mathbf{x}}^2 + \kappa^2 e^{i\psi_0(\mathbf{x}) + \phi(\mathbf{x})} \right] \delta(\mathbf{x} - \mathbf{y}), \quad (11)$$

is the second variation of the action  $\mathcal{S}[\psi, \phi]$ . Notice that the linear term in  $\Delta\psi(\mathbf{x})$  does not contribute to the expansion since  $\psi_0(\mathbf{x})$  satisfies the saddle-point equation Eq. (6). Performing the Gaussian integrals in Eq. (4), we obtain an expression for the change in the free energy due to fluctuations of the counterions:

$$\beta \Delta \mathcal{F} = \frac{1}{2} \ln \det \hat{\mathbf{K}} - \frac{1}{2} \ln \det [-\nabla_{\mathbf{x}}^2], \quad (12)$$

where the second term comes from the normalization factor  $\mathcal{N}_0$ . Thus, combining Eqs. (8) and (12) together, the

total electrostatic free energy of the system can be expressed as

$$\beta F_{el} = \beta F_0 + \frac{1}{2} \ln \det \hat{\mathbf{K}} - \frac{1}{2} \ln \det [-\nabla_{\mathbf{x}}^2]. \quad (13)$$

Thus, the total electrostatic free energy is comprised of a mean-field free energy and a fluctuating free energy. Note that the expansion parameter of the total free energy is proportional  $\kappa \ell_B$ , where  $1/\kappa$  roughly corresponds to the average distance between charges. Thus, for highly charged systems, the fluctuating term, linear in  $\kappa \ell_B$ , may become important, and the mean-field PB free energy no longer provides a reasonable approximation. The computation of the fluctuating free energy relies on diagonalizing the operator  $\hat{\mathbf{K}}(\mathbf{x}, \mathbf{y})$ , which depends on the mean-field solution. For counterions in a uniform background, this term gives the usual Debye-Hückel free energy,  $\Delta F/V = -k_B T \kappa^3 / (12\pi)$  [27]. However, it might be difficult to calculate this term in general, and exact evaluation is known only for planar systems [7, 28]. Indeed, as we will see below, an approximation must be introduced in order to compute this term analytically for our model of polyelectrolyte brush.

### III. SINGLE POLYELECTROLYTE BRUSH

We consider a polyelectrolyte brush (see Fig. 1), formed by a long intrinsically flexible charged polymers grafted at one end onto an impermeable planar surface and immersed in a salt-free solution. We consider the simple case of monodisperse polymers of degree of polymerization,  $N$ , of which a fraction  $f$  is charged, with grafting density  $\rho$ . We avoid the complicated issue of how electrostatics induces stiffness of the chains, and simply assume that the polymers are Gaussian chains, with Kuhn length  $a$  which is the same molecular size of the counterions.

In addition to the electrostatic free energy, we have to model the energetics of the polyelectrolyte brush, arising from elasticity and its interaction with the solvent. Within the Alexander-deGennes approximation [21], in which monomer density are assumed to be constant in a region of height  $h$ , all the chains are stretched by an equal amount and store an elastic energy per unit area of

$$\beta F_G / \mathcal{A} = \frac{3h^2}{2Na^2} \rho, \quad (14)$$

where  $\mathcal{A}$  is the area of the surface. The solvent quality is described in terms of the Flory-Huggins free energy per unit area [30]

$$\beta F_V / \mathcal{A} = \frac{v}{2} a^3 c^2 h + \frac{w}{6} a^6 c^3 h. \quad (15)$$

where  $c = N\rho/h$  is the average monomer density,  $v$  is the dimensionless excluded-volume parameter, which is

positive for good solvents and negative for poor solvent, and  $w$  is the third virial coefficient which is typically positive and of order unity. In the next subsection, we discuss the electrostatic free energy within our model of polyelectrolyte model, as outlined in Sec. II. In Sec. III B, we present the phase diagram of our model.

### A. Mean-field theory and fluctuation contribution

The fixed charge distribution for an Alexander-de Gennes polyelectrolyte brush is  $n_f(\mathbf{x}) = n_0 \tilde{\Theta}(z - h)$ , where  $n_0 = fc = Nf\rho/h$  and  $f$  is the fraction of monomers that are charged. The function  $\tilde{\Theta}(x) = 1 - \Theta(x)$ , where  $\Theta(x)$  is the Heaviside step function, which equals 1 when  $x > 0$  and 0 when  $x < 0$ . Due to translation invariance in the  $xy$ -plane, the PB equation, Eq. (7) can be written as

$$\frac{d^2\varphi(z)}{dz^2} + \kappa^2 e^{-\varphi(z)} = \frac{\ell_B n_0}{Z} \tilde{\Theta}(z - h). \quad (16)$$

Outside the brush ( $z > h$ ), the right-hand side of Eq. (16) is zero and its solution is the same as that of a charged plane held at a constant potential:

$$\varphi_{>}(z) = \varphi_h + 2 \ln \left[ 1 + \frac{z - h}{\lambda} \right], \quad z > h, \quad (17)$$

where  $\varphi_h$ , which will be determined below, is the potential at the brush height and  $\lambda$  is the Gouy-Chapmann length, determined by  $\lambda = \sqrt{2} e^{\varphi_h/2} / \kappa$ , which is a measure of the extent of how diffuse the counterion distribution is outside of the brush.

Inside the brush we must solve

$$\frac{d^2\varphi_{<}}{dz^2} + \kappa^2 e^{-\varphi_{<}} = \frac{\ell_B n_0}{Z}, \quad z < h. \quad (18)$$

Multiplying this equation with  $\varphi_{<}$ , integrating once, and imposing the boundary conditions that the potential and the electric field at the grafting surface be zero, “the constant of motion” is found to be  $-\kappa^2$ , and we have

$$\frac{1}{2} \left( \frac{d\varphi_{<}}{dz} \right)^2 = \kappa^2 [e^{-\varphi_{<}} - 1] + \frac{\ell_B n_0 \varphi_{<}}{Z}. \quad (19)$$

Using the continuity of the electric field and potential across the boundary at  $z = h$ , we find that  $\kappa^2$  is related to  $\varphi_h$  by

$$\kappa^2 = \frac{\ell_B n_0 \varphi_h}{Z} = \frac{2\varphi_h}{\xi h}, \quad (20)$$

where we have defined  $\xi \equiv 2Z/(\ell_B n_0 h)$ . Note that this length is independent of  $h$ . The electrostatic potential inside the brush,  $\varphi_{<}(z)$ , is determined implicitly by

$$\int_0^{\varphi_{<}} \frac{d\varphi'}{\sqrt{e^{-\varphi'} - 1 + \frac{\varphi'}{\varphi_h}}} \equiv \Delta[\varphi_{<}(z), \varphi_h] = 2\sqrt{\frac{\varphi_h}{\xi h}} z. \quad (21)$$

In particular, the potential at the brush height,  $\varphi_h$  is determined by the relation

$$\Delta[\varphi_h, \varphi_h] = 2\sqrt{\varphi_h \frac{h}{\xi}}. \quad (22)$$

In the weak charging limit, it gives  $\varphi_h \approx h/\xi \ll 1$ , and in the strong charging limit,  $\varphi_h \approx 1$ . Fig. 2 plots the counterion density. It is clear in the strong charging limit that while most of the counterions is in the brush, there are still some outside. This point will be crucial when we discuss the fluctuation contributions below.

The mean-field electrostatic free energy per unit area can be calculated straightforwardly using the solution described above and Eq. (8). The result is

$$\beta f_0 = \frac{Nf\rho}{Z} \ln \left( \frac{2\varphi_h a^3}{\ell_B \xi h} \right) - \frac{2\varphi_h}{\ell_B \xi} - \frac{4}{\ell_B} \sqrt{\frac{\varphi_h}{\xi h}} \left[ e^{-\frac{\varphi_h}{2}} + \frac{1}{2} \int_0^{\varphi_h} d\varphi \sqrt{e^{-\varphi} - 1 + \frac{\varphi}{\varphi_h}} \right], \quad (23)$$

where we have made use of the fact that the chemical potential is given by  $\mu = \ln [\varphi_h a^3 / (2\xi^2 \ell_B)]$ . In the mean-field picture, electrostatics contributes an outward pressure,  $\Pi_{\text{MF}}(h) = -\partial f_0 / \partial h$ , which scales as  $\Pi_{\text{MF}}(h) \sim 1/(\ell_B \xi h)$ , in the strong charging limit, and  $\Pi_{\text{MF}}(h) \sim 1/(\ell_B \xi^2)$  in the weak charging limit. Note that this mean-field pressure is always repulsive. Balance this electrostatic pressure against that arising from the elasticity of Eq. (14), we have  $h \approx \xi / \beta_{el}$ , for  $\beta_{el} \ll 1$  (strong charging) and  $h \approx \xi / \beta_{el}^2$ , for  $\beta_{el} \gg 1$  (weak charging), where we have defined an important dimensionless parameter  $\beta_{el} \equiv Z^{1/2} \xi / (Nf^{1/2} a)$ , which characterizes the importance of the elastic term compared to electrostatic pressure. These scaling regimes (as plotted in Fig. 3) are well-known as discussed in Ref. [12]. Here, we study

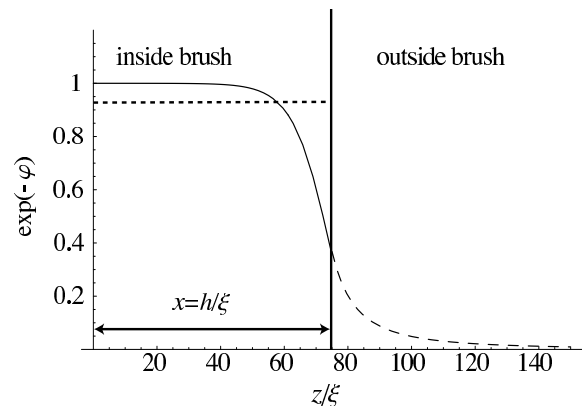


FIG. 2: A plot of the mean-field counterion density in the osmotic brush limit. It is clear that most of the counterion is trapped inside the brush. The dashed line represents the spatially averaged counterion density inside the brush [See, Eq. (27)]. This approximation is used to compute the fluctuation free energy.

deviations from these scaling laws when counterion fluctuations are taken into account.

To evaluate the fluctuation contribution to the free energy, we start with the expression for the change in the free energy due to fluctuations of the counterions, Eq. (12)

$$\beta\Delta\mathcal{F} = \frac{1}{2} \ln \det \hat{\mathbf{K}} - \frac{1}{2} \ln \det [-\nabla^2],$$

where the operator  $\hat{\mathbf{K}}$  for our model of polyelectrolyte brush is

$$\mathbf{K}(\mathbf{x}, \mathbf{y}) \equiv \left[ -\nabla_{\mathbf{x}}^2 + \kappa^2 e^{-\varphi} \tilde{\Theta}(z-h) + \frac{2\Theta(z-h)}{(z-h+\lambda)^2} \right] \delta(\mathbf{x}-\mathbf{y}). \quad (24)$$

The derivative of  $\Delta\mathcal{F}$  with respect to  $h$  can be straightforwardly calculated by making use of the exact identity  $\delta \ln \det \hat{\mathbf{X}} = \text{Tr} \hat{\mathbf{X}}^{-1} \delta \hat{\mathbf{X}}$ :

$$\begin{aligned} \frac{\partial \beta\Delta\mathcal{F}}{\partial h} &= \frac{1}{2\ell_B} \int d^3\mathbf{x} G(\mathbf{x}, \mathbf{x}) \\ &\times \frac{\partial}{\partial h} \left[ \kappa^2 e^{-\varphi} \tilde{\Theta}(z-h) + \frac{2\Theta(z-h)}{(z-h+\lambda)^2} \right], \end{aligned} \quad (25)$$

where  $G(\mathbf{x}, \mathbf{x})$  is the Green's function (inverse) of  $\mathbf{K}(\mathbf{x}, \mathbf{y})$  satisfying

$$\left[ -\nabla_{\mathbf{x}}^2 + \kappa^2 e^{-\varphi} \tilde{\Theta}(z-h) + \frac{2\Theta(z-h)}{(z-h+\lambda)^2} \right] G(\mathbf{x}, \mathbf{x}') = \ell_B \delta(\mathbf{x}-\mathbf{x}'). \quad (26)$$

Unfortunately,  $G(\mathbf{x}, \mathbf{x}')$  cannot be evaluated analytically because the counterion density inside the brush is not an explicit function of  $z$  [see Eq. (21)]. In order to make analytical progress, we employ the reasonable approximation that the counterion density inside the brush is a constant averaged over the brush, given by

$$\Lambda^2 \equiv \frac{1}{h} \int_0^h dz \kappa^2 e^{-\varphi(z)} = \frac{2}{\xi h} \left( 1 - \frac{\xi}{\lambda} \right). \quad (27)$$

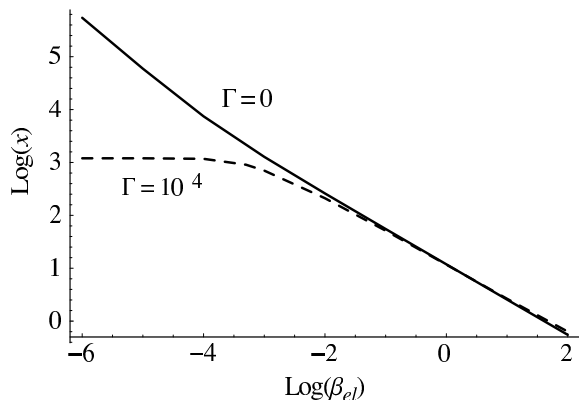


FIG. 3: The height versus beta for values of  $\Gamma = 0, 10^4$ .

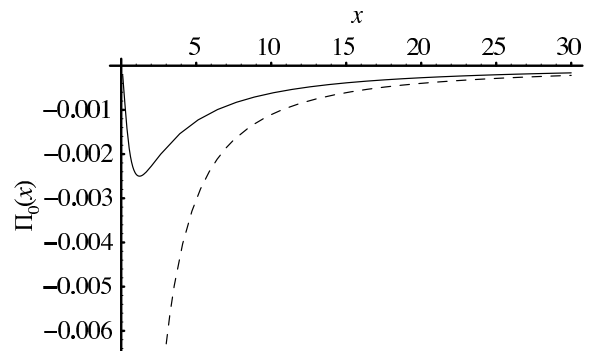


FIG. 4: The fluctuation contribution to the free energy,  $\Pi_0(x)$  (solid line), where  $x = h/\xi$  is the rescaled height variable. The scaling prediction for the fluctuation pressure from equation (29) (dashed line) diverges as small  $x$ .

This approximation entails neglecting the spatial variations inside the brush. Judging from Fig. 2, this approximation should not be in serious error.

Within this approximation,  $G(\mathbf{x}, \mathbf{x}')$  can be evaluated analytically (see Appendix), and we find

$$\begin{aligned} \frac{1}{\mathcal{A}} \frac{\partial \beta\Delta\mathcal{F}}{\partial h} &= \frac{\Lambda^2}{h} [\mathcal{I}_1(h) - \mathcal{I}_2(h)] + \frac{\mathcal{I}_5(h)}{h^3} \\ &+ \frac{1}{\lambda^2 h} \frac{\partial \lambda}{\partial h} [\mathcal{I}_3(h) - \mathcal{I}_4(h) + 2\mathcal{I}_2(h)], \end{aligned} \quad (28)$$

where the dimensionless integrals  $\mathcal{I}_i(h)$  are defined in the Appendix. This is the main result of this paper. It says that counterion fluctuations contribute an inward (negative) pressure  $\Pi_f(h) = -\mathcal{A}^{-1} \partial \Delta\mathcal{F} / \partial h \equiv \Gamma \xi^{-3} \Pi_0(h/\xi)$ , as plotted in Fig. 4. First, the fact that it is negative is consistent with the notion that the fluctuations must lower the free energy. The strength of this pressure is controlled by  $\Gamma = \ell_B/\xi$ , which roughly scales as  $(\ell_B f \rho)^2$ . Thus, this term becomes important for highly charged polyelectrolytes, as expected.

Although the expression Eq. (28) looks rather complicated, we can understand its meaning by expanding  $\Pi_0(h/\xi)$  in the strong charging limit:

$$\begin{aligned} \Pi_0(h/\xi) &= -\alpha_1 (\xi/h)^{3/2} + \alpha_2 (\xi/h)^2 \\ &- \alpha_3 (\xi/h)^{5/2} + \dots, \end{aligned} \quad (29)$$

where  $\alpha_1 \sim 0.0375$  and  $\alpha_2 \sim 0.00833$  are constants. The first term is the fluctuation contribution to the free energy of a coulomb gas of counterions distributed uniformly throughout the brush volume. To see this, recall that in the strong charging limit most of the counterions is within the brush, with a 3D concentration of  $c \sim n_0/h$ . This implies that the inverse of the 3D “screening” length  $\kappa_s \sim \sqrt{\ell_B n_0/h}$ . Using the Debye-Hückel free energy (per unit volume)  $\beta\Delta f \sim -\kappa_s^3$ , we have  $\Pi_f(h) \sim \partial(\Delta f \cdot h) / \partial h \sim h^{-3/2}$ , which is the first term in Eq. (29). In fact, similar argument has been used by Csajka *et al.* [26] to derive the scaling laws. The second term in Eq. (29) may be interpreted as an effective

second virial term arising from the coupling between fluctuations of the counterions inside the brush and outside. Note that this term is not included in the scaling theory for collapsed brushes. It is interesting to note that the divergence at small  $h$  of the asymptotic fluctuation pressure is purely an artifact of the approximation, and it is not present in Eq. (28). It is likely then that scaling laws derived for the collapsed state of a polyelectrolyte brush using similar approximate expressions may not capture the full behavior of the brush.

## B. Phase Diagram

Now, we are in the position to discuss the equilibrium phase diagram of the polyelectrolyte brush. The important quantity, the equilibrium height of the brush, is determined by minimizing the total free energy of the polyelectrolyte brush,  $F = F_G + F_V + F_{el}$ , with respect to the brush height. It is more convenient to employ the following dimensionless variables:

$$\omega \equiv N\rho a^2 \quad (30)$$

$$\nu \equiv \frac{va^3 Z^2}{\ell_B \xi^2 f^2}. \quad (31)$$

in addition to  $x \equiv h/\xi$ ,  $\Gamma \equiv \ell_B/\xi$ , and  $\beta_{el} \equiv Z^{1/2}\xi/(Nf^{1/2}a)$  already defined in the previous section. The variable  $\nu$  is a measure of the contribution to the pressure from the second virial coefficient compared to the mean field pressure. Note that the mean-field pressure and the fluctuation pressure depends on  $x$  only.

In Fig. 5, we display the typical phase diagram of a polyelectrolyte brush in contact with a theta solvent as a function of  $\beta_{el}$  and  $\Gamma$ . We find a first order collapse transition line, from the osmotic brush to the collapse brush, represented by the solid line in Fig. 5. This line terminates at a critical point, which is well within the strong charging regime,  $\beta_{el} < 1$ . Thus, it is similar to the liquid-gas transition. This behavior resembles to that of a polyelectrolyte brush in a poor solvent, where attractive interaction between monomers mediated by the solvent acts against the electrostatic repulsion to collapse the brush [13]. Here, fluctuations induce an attractive interaction which collapse the brush. This effect on the brush height can be clearly seen in Fig. 3. It is interesting to note that the valence of the counterions plays a crucial role. For typical brushes, increasing the charge fraction while holding other parameters fixed (as shown with dotted lines in Fig. 5), only the monovalent counterion goes through the first-order collapse. For divalent and trivalent counterions, on the other hand, we observe a smooth continuous decrease in  $h$ , as shown in Fig. 6, where we plot the brush height as a function of the charge fraction  $f$ . As expected, correlation effects are more important for higher valence  $Z$  of the counterions. Even for a moderately charge fraction  $f$ , the brush height already starts to decrease for for divalent and trivalent counterions. It

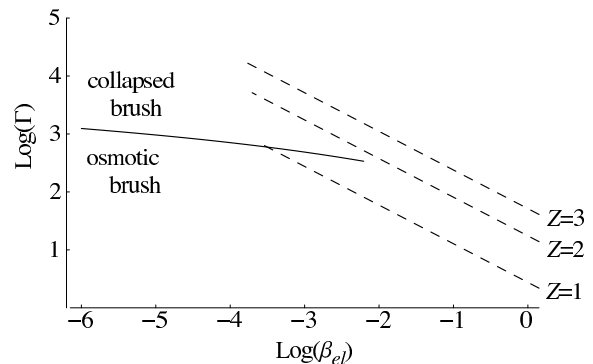


FIG. 5: Typical phase diagram of a single brush in theta solvent (in this case,  $N = 200$ ,  $\omega = 1$ ). The solid line represents a first order phase transition between the osmotic brush and the collapsed brush regimes. The Pincus brush regime occurs for  $\beta \approx 1$  and is not shown. The dashed curves are generated holding all parameters constant except the brush charge fraction (arrows indicate increasing charge fraction) for monovalent, divalent, and trivalent counterions.

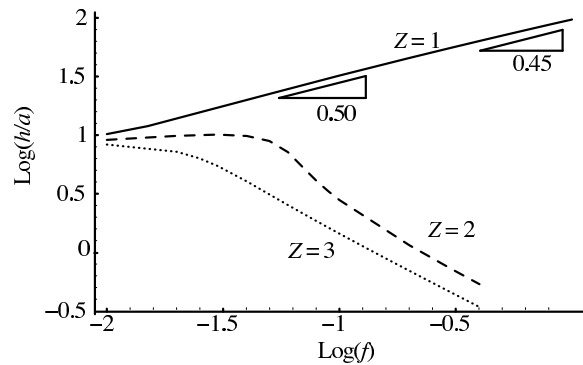


FIG. 6: Brush height for monovalent (solid), divalent (dashed), and trivalent (dotted) counterions in a theta solvent (see figure 5). The monovalent salt height obeys the power law  $h \propto f^{0.50}$ , though it shows minor deviations from power at very strong charging (with an exponent  $\approx 0.45$ ).

is also interesting to observe that for monovalent counterion (before the collapse transition), the brush height obeys the osmotic brush scaling law of  $h \sim f^{1/2}$  only for moderate  $f$ , which crosses over to  $h \sim f^{0.45}$ . Deep inside the collapsed regime, the brush height is determined by the fluctuation pressure against the third virial term, which gives  $h \sim \omega^2 \xi / \Gamma^{2/3} \sim f^{-5/3}$ . This is not shown in Fig. 6.

In a good solvent, the polyelectrolyte brushes do not show any major qualitative difference from a theta solvent. A typical phase diagram is shown in Fig. 7. In this case, the first-order phase boundary occurs at higher values of  $\epsilon$  and the critical point shifts to even smaller values of  $\beta_{el}$ . This is not surprising because in a good solvent, there is an additional outward pressure which the fluctuation pressure must overcome before the brush is collapsed. In addition, it is interesting to observe in Fig. 8,

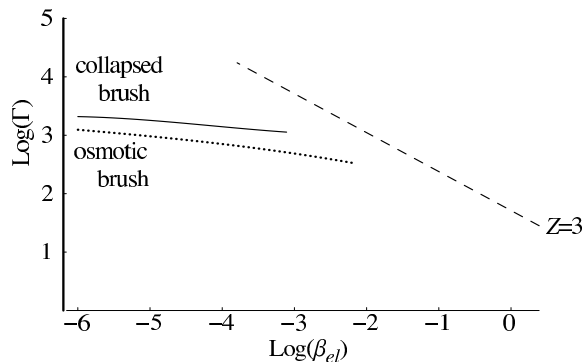


FIG. 7: Typical phase diagram for good solvent ( $v = 17.0275$ ,  $Z = 3$ ) for the brush of figure 5. The solid line is a first order phase transition from the osmotic to collapsed brush regimes. For comparison, the transition for a brush in theta solvent is shown by the dotted line. Notice that in good solvent, the transition line occurs at higher values of  $\epsilon$  and the critical point occurs for smaller values of  $\beta_{el}$ . This is also typical of brushes with large values of  $\omega$ . As a further reference, the dashed line shows the curve of increasing charge fraction in for trivalent salt. For the case of monovalent counterions, the first-order transition occurs for smaller values of  $\epsilon$  than with trivalent counterions.

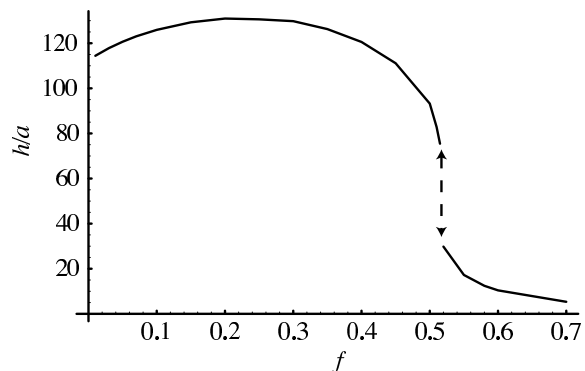


FIG. 8: Brush height vs. charge fraction in good solvent for monovalent counterions at high density ( $\rho a^2 = 0.0625$ ).

where we have plotted the behavior of the brush height as a function of the charge fraction, that the brush height increases at low charge fraction, then decreases with increasing charge fraction, and eventually collapse. This nonmonotonic behavior is qualitatively similar to that observed by Bendejacq *et al.* [24] for monovalent salt in highly charged and dense cylindrical brushes.

For an osmotic brush at the level of a scaling theory, the brush height is independent of the grafting density. In theta solvent, significant deviations from osmotic brush scaling can be seen even for monovalent counterions as well as a discontinuous collapse (see dotted curve in Fig. 9). In good solvent, however, the brush height scales nearly linear in the grafting density, as shown in Fig. 9. This scaling can be understood from balancing of the second virial pressure against the fluctuation pressure:

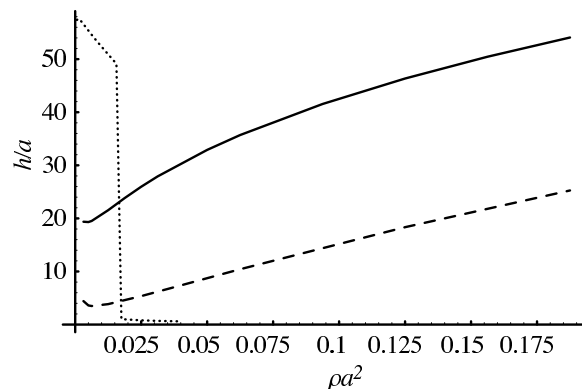


FIG. 9: Brush height vs. density ( $N = 200$ ,  $f = 0.3$ ). In theta solvent (dotted curve), the brush height exhibits a first order collapse. In good solvent for monovalent (solid) and divalent (dashed) counterions, the brush height decreases initially, then increases. At large densities, the increase is linear.

$$h \sim \xi \omega^4 [v \xi / (\Gamma a)]^2 \sim \rho.$$

#### IV. CONCLUDING REMARKS

In this paper, we have shown that expanding the counterion free energy systematically about Poisson-Boltzmann mean field theory for a single brush results in a collapse transition of the brush height with multivalent counterions. Though we find a first order transition similar to that of Csajka *et al.* [26], we also find a critical point in the phase diagram and find that, generically, the decrease in brush height is continuous.

The major difference in formulation between our theory and this scaling theory is that the fluctuations of counterions outside of the brush have been taken into account at the quadratic level. Fluctuations of counterions from the interior to exterior region of the brush are likely to be responsible for the existence of the critical point in the phase diagram.

Throughout this paper, we have assumed that all chains in the brush are equally stretched, and that the monomer density is constant throughout the brush. We have also employed the constant density approximation for the counterion density within the brush when expanding in the fluctuations. These approximations have been necessary in order to calculate the fluctuation pressure, though in reality the monomer density is known to be approximately parabolic [32]. It is possible that the discontinuity of monomer density in our approximation is responsible for the first order transition region, and that a more exact theory may have a critical point at much smaller values of  $\beta_{el}$  or no first order transition at all [33].

Neglected in our treatment is fluctuations of the polyelectrolyte chains themselves. These corrections to the free energy are likely to be unimportant if the fluctuations of uncondensed counterions do not couple strongly

to them. They may play a role, however, when condensed counterions are properly taken into account.

We have also neglected the inhomogeneities of the monomer density in the brush, which induces inhomogeneities in the mean field counterion density. These inhomogeneities are due, in part, to counterion condensation on the polyelectrolyte chains. These condensed counterions are not free to fluctuate and do not contribute to the osmotic pressure due to the counterion entropy. Further, the condensed counterions can cause additional attractions between the chains of the brush due to structural correlations beyond those calculated in this paper.

In future work, we will study the problem of attractive interactions between two opposing brushes, and work to understand more precisely the role of condensed counterions in the brush.

### Acknowledgments

We acknowledge discussions with D. Bendejacq, V. Ponsinet, and in particular T.C. Lubensky and P. Pin-

cus for a critical reading of the manuscript and indispensable input for this work to take shape. CDS is supported through the NSF Grant DMR 02-03755 and the MRL Program of the National Science Foundation under Award No. DMR 00-80034. AWC acknowledges supports from NSF through the MRSEC Grant DMR 00-79909.

### APPENDIX A: CALCULATION OF FLUCTUATION ENERGY FOR A SINGLE BRUSH

Within the constant counterion density approximation within the brush, the Fourier transform of  $G(\mathbf{x}, \mathbf{x}')$  in the  $xy$ -plane,  $G(z, z'; q)$ , satisfies

$$\left[ -\frac{\partial^2}{\partial z^2} + q^2 + \Lambda^2 \tilde{\Theta}(z-h) + \frac{2\Theta(z-h)}{(z-h+\lambda)^2} \right] G(z, z'; q) = \ell_B \delta(z-z'), \quad (\text{A1})$$

where  $\Lambda^2 \equiv 2(1-\xi/\lambda)/(\xi h)$ , and can be solved by standard technique [34]. The result is

$$G_{<}(z, z; q) = \frac{\ell_B}{2\alpha} \frac{[e^{-\alpha z} - \mathcal{M}_1(q)e^{+\alpha z}][e^{+\alpha z} + \mathcal{M}_2(q)e^{-\alpha z}]}{1 + \mathcal{M}_1(q)\mathcal{M}_2(q)}, \quad \text{for } z < h, \quad (\text{A2})$$

$$G_{>}(z, z; q) = \frac{\ell_B}{2q} \left[ 1 - \frac{1}{q^2(z-h+\lambda)^2} \right] + \frac{\ell_B \mathcal{L}(q) e^{-2q(z-h)}}{2q} \left[ 1 + \frac{1}{q(z-h+\lambda)} \right]^2, \quad \text{for } z > h, \quad (\text{A3})$$

$$\mathcal{L}(q) \equiv \frac{[1 - q\lambda(1-q\lambda)] \{1 + f_-(q) + \mathcal{M}_2(q)e^{-2\alpha h} [1 - f_-(q)]\}}{[1 + q\lambda(1+q\lambda)] \{1 + f_+(q) + \mathcal{M}_2(q)e^{-2\alpha h} [1 - f_+(q)]\}}, \quad (\text{A4})$$

where  $\alpha^2 = q^2 + \Lambda^2$ ,  $\mathcal{M}_1(q) \equiv e^{-2\alpha h} \left[ \frac{1-f_+(q)}{1+f_+(q)} \right]$ ,  $\mathcal{M}_2(q) \equiv (\alpha - q)/(\alpha + q)$ , and  $f_{\pm} \equiv \alpha\lambda(1 \pm q\lambda)/[1 \pm q\lambda(1 \pm q\lambda)]$ . Now, returning to the expression of the derivative of  $\Delta\mathcal{F}$  with respect to  $h$ , Eq. (25), by noting that the derivative of  $\partial\Theta(z-h)/\partial h = -\delta(z-h)$  and  $\partial\tilde{\Theta}(z-h)/\partial h = +\delta(z-h)$ , we find that Eq. (25) consists of three parts:

$$\frac{1}{\mathcal{A}} \frac{\partial\Delta\mathcal{F}}{\partial h} = \frac{1}{\mathcal{A}} \frac{\partial\Delta\mathcal{F}_1}{\partial h} + \frac{1}{\mathcal{A}} \frac{\partial\Delta\mathcal{F}_2}{\partial h} + \frac{1}{\mathcal{A}} \frac{\partial\Delta\mathcal{F}_3}{\partial h}, \quad (\text{A5})$$

where  $\mathcal{A}$  is the area of the plane and

$$\begin{aligned} \frac{1}{\mathcal{A}} \frac{\partial\beta\Delta\mathcal{F}_1}{\partial h} &= \int \frac{d^2\mathbf{q}}{(2\pi)^2} \int_0^h \frac{dz}{2\ell_B} G_{<}(z, z, q) \frac{\partial\Lambda^2}{\partial h} \\ \frac{1}{\mathcal{A}} \frac{\partial\beta\Delta\mathcal{F}_2}{\partial h} &= \int \frac{d^2\mathbf{q}}{(2\pi)^2} \int_h^\infty \frac{dz}{2\ell_B} G_{>}(z, z, q) \frac{\partial}{\partial h} \left[ \frac{2}{(z-h+\lambda)^2} \right], \\ \frac{1}{\mathcal{A}} \frac{\partial\beta\Delta\mathcal{F}_3}{\partial h} &= \left( \Lambda^2 - \frac{2}{\lambda^2} \right) \int \frac{d^2\mathbf{q}}{(2\pi)^2} \frac{G(h, h, q)}{2\ell_B}. \end{aligned} \quad (\text{A6})$$

After lengthy algebra, we have

$$\frac{1}{\mathcal{A}} \frac{\partial\Delta\mathcal{F}}{\partial h} = \frac{\Lambda^2}{h} [\mathcal{I}_1(h) - \mathcal{I}_2(h)] + \frac{1}{\lambda^2 h} \frac{\partial\lambda}{\partial h} [\mathcal{I}_3(h) - \mathcal{I}_4(h) + 2\mathcal{I}_2(h)] + \frac{\mathcal{I}_5(h)}{h^3}, \quad (\text{A7})$$

where the dimensionless integrals  $\mathcal{I}_i(h)$  are defined as

$$\mathcal{I}_1(h) \equiv h \int \frac{d^2\mathbf{q}}{(2\pi)^2} \frac{1}{4\alpha} \left\{ \frac{\mathcal{M}_2(q)e^{-2\alpha h}}{1 + \mathcal{M}_1(q)\mathcal{M}_2(q)} - \frac{1 - f_+(q)}{[1 + f_+(q)][1 + \mathcal{M}_1(q)\mathcal{M}_2(q)]} \right\}, \quad (\text{A8})$$



$$\mathcal{I}_2(h) \equiv \int \frac{d^2\mathbf{q}}{(2\pi)^2} \frac{1}{8\alpha^2} \frac{1 - e^{-2\alpha h}}{1 + \mathcal{M}_1(q)\mathcal{M}_2(q)} \left[ \mathcal{M}_2(q) - \frac{1 - f_+(q)}{1 + f_+(q)} \right], \quad (\text{A9})$$

$$\mathcal{I}_3(h) \equiv h \int \frac{d^2\mathbf{q}}{(2\pi)^2} \frac{1}{2\alpha} \left[ 1 - \frac{\alpha}{q} - \frac{2\mathcal{M}_1(q)\mathcal{M}_2(q)}{1 + \mathcal{M}_1(q)\mathcal{M}_2(q)} \right], \quad (\text{A10})$$

$$\mathcal{I}_4(h) \equiv h \int \frac{d^2\mathbf{q}}{(2\pi)^2} \frac{1}{2q} \frac{1 + \lambda(\alpha - q) + \mathcal{M}_2(q)e^{-2\alpha h} [1 + \lambda(\alpha + q)]}{[1 + q\lambda + q^2\lambda^2 + \alpha\lambda(1 + q\lambda)] [1 + \mathcal{M}_1(q)\mathcal{M}_2(q)]} \quad (\text{A11})$$

$$\mathcal{I}_5(h) \equiv \frac{h^3}{2} \int \frac{d^2\mathbf{q}}{(2\pi)^2} \frac{(\alpha - q) [1 - e^{-2\alpha h}]}{[1 + q\lambda + q^2\lambda^2 + \alpha\lambda(1 + q\lambda)] [1 + \mathcal{M}_1(q)\mathcal{M}_2(q)]}. \quad (\text{A12})$$

- [1] A.Yu.Groberg, T.T. Nguyen, and B.I. Shklovskii, *Rev. Mod. Phys.* **74**, 329 (2002).
- [2] Yan Levin, *Rep. Prog. Phys.* **65**, 1577 (2002).
- [3] A.G. Moreira and Roland R. Netz, in *Electrostatic Effects in Soft Matter and Biophysics*, edited by C. Holm, P. Kikicheff, and R. Podgornik (Kluwer Acad. Pub., Boston, 2001).
- [4] J.N. Israelachvili, *Intermolecular and Surface Forces*. (Academic Press Inc., San Diego, 1992).
- [5] B.-Y Ha and A.J. Liu, *Phys. Rev. Lett.* **79**, 1289 (1997); *Phys. Rev. Lett.* **81**, 1011 (1998); *Phys. Rev. E* **58**, 6281 (1998); *Phys. Rev. E* **60**, 803 (1999).
- [6] P. Pincus and S.A. Safran, *Europhys. Lett.* **42** 103 (1998); D.B. Lukatsky and S.A. Safran, *Phys. Rev. E* **60**, 5848 (1999).
- [7] A.W.C. Lau, P. Pincus, *Phys. Rev. E* **66**, 041501 (2002).
- [8] R. Golestanian, M. Kardar, and T.B. Liverpool, *Phys. Rev. Lett.* **82**, 4456 (1999); R. Golestanian, T.B. Liverpool, *Phys. Rev. E* **66**, 051802 (2002).
- [9] H. Schiessel and P. Pincus, *Macromolecules* **31**, 7953 (1998).
- [10] S.J. Miklavic, S. Marcelja, *J. Phys. Chem.* **92**, 6718 (1988).
- [11] S. Misra, S. Varanasi, P.P. Varanasi, *Macromolecules*, **22** 5173 (1989).
- [12] P. Pincus, *Macromolecules* **24**, 2912 (1991).
- [13] R.S. Ross, P. Pincus, *Macromolecules* **25**, 2177 (1992); E.B. Zhulina, T.M. Birshtein, and O.V. Borisov, *J. Phys. II* **2**, 63 (1992).
- [14] O.V. Borisov, T.M. Birshtein, and E.B. Zhulina, *J. Phys. II* **1**, 521 (1991); R. Israel, F.A.M. Leermakers, G.J. Fleer, E.B. Zhulina, *Macromolecules* **27**, 3249 (1994); O.V. Borisov, E.B. Zhulina, T.M. Birshtein, *Macromolecules* **27**, 4795 (1994);
- [15] E.B. Zhulina, O.V. Borisov, *J. Chem. Phys.* **107**, 5952 (1997); E.B. Zhulina, J. Klein Wolterink, O.V. Borisov, *Macromolecules* **33**, 4945 (2000).
- [16] J. Wittmer, J.-F. Joanny, *Macromolecules* **26**, 2691 (1993).
- [17] C. Amiel, M. Sikka, J.W. Schneider, Jr., Y.-H. Tsao, M. Tirrell, and J.W. Mays, *Macromolecules* **28**, 3125 (1995); T.W. Kelley, P.A. Schorr, K.P. Johnson, M. Tirrell, C.D. Frisbie, *Macromolecules* **31**, 4297 (1998)
- [18] Y. Mir, P. Auvroy, L. Auvray, *Phys. Rev. Lett.* **75**, 2863 (1995).
- [19] P. Guenoun, A. Schlachli, D. Sentenac, J.M. Mays, J.J. Benattar, *Phys. Rev. Lett.* **74**, 3628 (1995).
- [20] H. Ahrens, S. Forster, C.A. Helm, *Macromolecules* **30**, 8447 (1997); *Phys. Rev. Lett.* **81** 4172 (1998).
- [21] S. Alexander, *J. Phys. (France)* **38** 983 (1997); P.G. de Gennes, *Macromolecules* **13**, 1069 (1980).
- [22] M.N. Tamashiro, E. Hernandez-Zapata, P.A. Schorr, M. Balastre, M. Tirrell, P. Pincus, *J. Chem. Phys.* **115** 1960 (2001); M. Balastre, F. Li, P. Schorr, J. Yang, J. Mays, M. Tirrell, *Macromolecules* **35** 9480 (2002).
- [23] P.A. Schorr, Ph.D. Thesis, University of Minnesota, 2000.
- [24] D. Bendejacq, Ph.D. Thesis, University of Paris, 2002.
- [25] F.S. Csajka, C. Seidel, *Macromolecules* **4**, 505 (2001); C. Seidel, *Macromolecules* **36**, 2536 (2003).
- [26] F.S. Csajka, R.R. Netz, C. Seidel, J.-F. Joanny, *Eur. Phys. J. E* **4**, 505 (2001).
- [27] L.D. Landau and E.M. Lifshitz, *Statistical Physics*, (Pergamon, New York, 1980), 3rd ed., rev. and enl. by E.M. Lifshitz and L.P. Pitaevskii.
- [28] A.W.C. Lau, D.B. Lukatsky, P.Pincus, and S. Safran, *Phys. Rev. E* **5**, 051502 (2002).
- [29] R.R. Netz, H. Orland, *Eur. Phys. J. E* **1**, 67 (2000).
- [30] de Gennes, P.-G. *Scaling Concepts in Polymer Physics*; Cornell University Press: Ithaca, NY, 1979.
- [31] S.T. Milner, T.A. Witten, M.E. Cates, *Europhys. Lett.* **5**, 413 (1988); *Macromolecules* **21**, 610 (1988); S.T. Milner, *Science* **251**, 905 (1991).
- [32] A.M. Skvortsov, I.V. Pavlushkov, A.A. Gorbunov, Y.B. Zhulina, O.V. Borisov, V.A. Pryamitsyn, *Polym. Sci.* **30** 17, 1706 (1988).
- [33] A. Halperin, *J. Phys. (France)* **49**, 547 (1988); Y.B. Zhulina, V.A. Pryamitsyn, O.V. Borisov, *Polym. Sci.* **31** 205 (1989); E.B. Zhulina, O.V. Borisov, V.A. Pryamitsyn, T.M. Birshtein, *Macromolecules* **24**, 140 (1991); D.R.M. Williams, *J. Phys. II (France)* **3**, 1313 (1993).
- [34] G. Arfken, *Mathematical Methods for Physicists* (Academic Press, San Diego, 1996).